Conjugated Porphyrin Ladders

Harry L. Anderson†

University Chemical Laboratory, Lensfield Road, Cambridge CB2 1EW, U.K.

Received November 11, 1993®

A conjugated porphyrin dimer has been synthesized from a *meso*-diethynylporphyrin. The zinc complex of the dimer aggregates much more strongly (K_{Agg} = 1.2 × 10^7 M^{-1}) than its analogous monomer (K_{Agg} = 3.8 × 10^2 M^{-1}) and forms a very stable 2:2 ladder complex with 1,4-diazabicyclo[2.2.2]octane (K_F = 4 × 10^{21} M^{-3}), which is in slow exchange on the NMR time scale at 30 °C. The effective molarities for aggregation and ladder formation are 80 and 0.3 M, respectively. NMR ring current shifts and UV exciton coupling show that the porphyrins are coplanar in the aggregate. The HOMO–LUMO gap for the dimer (1.7 eV) is 0.2 eV less than that of the monomer and the exciton splitting in the dimer is extraordinarily large (76 nm), implying substantial electronic overlap between the chromophores.

Molecules with very long π-systems are of intense interest as organic semiconductors,[1] near-IR dyes[2] and third-order nonlinear optical materials.[3] They can be built as ribbons of simple chromophores; the problem is how to hold the π-systems coplanar within a ribbon, to maximize π-overlap. One solution is to fuse the units edge-to-edge, to make a covalent ladder polymer, but this is synthetically demanding. An alternative strategy is to hold the chromophores coplanar noncovalently, by forming a self-assembling ladder. The three-dimensional structures of most biopolymers are controlled by noncovalent interactions, either between different parts of the same strand (as in protein α-helices and starch) or between two separate strands (as in the DNA duplex and protein β-sheet). Such interactions must also be capable of controlling the conformation of synthetic polymers, yet this idea appears to have received little attention.[4]

Porphyrins are intriguing units from which to construct conjugated polymers. Many linear porphyrin and phthalocyanine oligomers have been synthesized,[5-26] but most do not allow conjugation between the macrocycles. This paper develops an approach to a *meso*-butadiyne linked porphyrin polymer, Zn_n**1**, and presents work on a dimeric model compound, Zn_2**2**. The

† Present address: Laboratorium für Organische Chemie, ETH-Zentrum, Universitätstrasse 16, CH-8092 Zürich, Switzerland.

® Abstract published in *Advance ACS Abstracts,* January 15, 1994.

(1) *Conjugated Polymeric Materials: Opportunities in Electronics, Optoelectronics and Molecular Electronics*; Brédas, J. L., Chance, R. R., Eds.; NATO ASI Series E 182; Kluwer Academic: Dordrecht, The Netherlands, 1990.

(2) Fabian, J.; Nakazumi, H.; Matsuoka, M. *Chem. Rev.* **1992**, *92*, 1197–1226.

(3) Nalwa, H. S. *Adv. Mater.* **1993**, *5*, 341–358.

(4) Analogues of DNA with hexose instead of pentose sugars have been synthesized: Böhringer, M.; Roth, H.-J.; Hunziker, J.; Göbel, M.; Krishnan, R.; Giger, A.; Schweizer, B.; Schreiber, J.; Leuman, C.; Eschenmoser, A. *Helv. Chim. Acta* **1992**, *75*, 1416–1477. Double and triple helical oligopyridine complexes have also been developed: Krämer, R.; Lehn, J.-M.; DeCian, A.; Fischer, J. *Angew. Chem., Int. Ed. Engl.* **1993**, *32*, 703–706. Constable, E. C. *Angew. Chem., Int. Ed. Engl.* **1991**, *30*, 1450–1451. Aggregation is thought to account for the properties of many polymers in solution, such as the solvatochromism of soluble polydiacetylenes and poly(3-alkyl)thiophenes: Chu, B.; Xu, R. *Acc. Chem. Res.* **1991**, *24*, 384–389. Rughooputh, S. D. D. V.; Hotta, S.; Heeger, A. J.; Wudl, F. J. *Polym. Sci. Polym. Phys. Ed.* **1987**, *25*, 1071–1078. However polymer aggregation is poorly understood. Polyrotaxanes are a simpler example of supramolecular polymers: Harada, A.; Li, J.; Kamachi, M. *Nature (London)* **1992**, *356*, 325–327. Wenz, G.; Keller, B. *Angew. Chem., Int. Ed. Engl.* **1992**, *31*, 197–199. Stoddart, J. F. *Angew. Chem., Int. Ed. Engl.* **1992**, *31*, 846–847.

(5) References 6–25 cover recent work on noncyclic porphyrin oligomers; only a few of these systems[8,19b,25] are conjugated. Coordination-linked porphyrin and phthalocyanine oligomers have also been studied extensively and often have electronically delocalized structures; for recent reviews see: Kellog, E.; Gaudiello, J. G. In *Inorganic Materials*; Bruce, D. W., O'Hare, D., Eds.; Wiley: Chichester, 1992; pp 353–396. Marks, T. J. *Angew. Chem., Int. Ed. Engl.* **1990**, *29*, 857–879. Hanack, M.; Deger, S.; Lange, A. *Coord. Chem. Rev.* **1988**, *83*, 115–136.

(6) (a) Sessler, J. L.; Johnson, M. R.; Creager, S. E.; Fettinger, J. C.; Ibers, J. A. *J. Am. Chem. Soc.* **1990**, *112*, 9310–9329. (b) Sessler, J. L.; Capuano, V. L. *Angew. Chem., Int. Ed. Engl.* **1990**, *29*, 1134–1137. Sessler, J. L.; Johnson, M. R.; Lin, T.-Y. *Tetrahedron* **1989**, *45*, 4767–4784. (c) Won, Y.; Friesner, R. A.; Johnson, M. R.; Sessler, J. L. *Photosynth. Res.* **1989**, *22*, 201–210.

(7) Helms, A.; Heiler, D.; McLendon, G. *J. Am. Chem. Soc.* **1992**, *114*, 6227–6238. Helms, A.; Heiler, D.; McLendon, G. *J. Am. Chem. Soc.* **1991**, *113*, 4325–4327. McLendon, G. *Acc. Chem. Res.* **1988**, *21*, 160–167.

(8) (a) Arnold, D. P.; Nitschinsk, L. J. *Tetrahedron Lett.* **1993**, *34*, 693–696. (b) Arnold, D. P.; Nitschinsk, L. J. *Tetrahedron* **1992**, *48*, 8781–8792. (c) Arnold, D. P.; Johnson, A. W.; Mahendran, M. *J. Chem. Soc., Perkin Trans. 1* **1978**, 336–370.

(9) Wasielewski, M. R. *Chem. Rev.* **1992**, *92*, 435–461. Wasielewski, M. R.; Johnson, D. G.; Niemczyk, M. P.; Gaines, G. L.; O'Neil, M. P.; Svec, W. A. *J. Am. Chem. Soc.* **1990**, *112*, 6482–6488.

(10) (a) Osuka, A.; Kobayashi, F.; Nakajima, S.; Maruyama, K.; Yamzaki, I.; Nishimura, Y. *Chem. Lett.* **1993**, 161–164. Osuka, A.; Kobayashi, F.; Maruyama, K.; Mataga, N.; Asahi, T.; Okada, T.; Yamzaki, I.; Nishimura, Y. *Chem. Phys. Lett.* **1993**, *201*, 223–228. Osuka, A.; Nakajima, S.; Maruyama, K. *J. Org. Chem.* **1992**, *57*, 7355–7359. Osuka, A.; Nakajima, S.; Nagata, T.; Maruyama, K.; Toriumi, K. *Angew. Chem., Int. Ed. Engl.* **1991**, *30*, 582–584. Osuka, A.; Maruyama, K.; Mataga, N.; Asahi, T.; Yamazaki, I.; Tamai, N. *J. Am. Chem. Soc.* **1990**, *112*, 4958–4959. (b) Nagata, T.; Osuka, A.; Maruyama, K. *J. Am. Chem. Soc.* **1990**, *112*, 3054–3095. Osuka, A.; Maruyama, K. *J. Am. Chem. Soc.* **1988**, *110*, 4454–4456.

(11) (a) Hammel, D.; Erk, P.; Schuler, B.; Heinze, J.; Müllen, K. *Adv. Mater.* **1992**, *4*, 737–739. (b) Hammel, D.; Kautz, C.; Müllen, K. *Chem. Ber.* **1990**, *123*, 1353–1356. Cosmo, R.; Kautz, C.; Meerholz, K.; Heinze, J.; Müllen, K. *Angew. Chem., Int. Ed. Engl.* **1989**, *28*, 604–607.

(12) Ponomarev, G. V.; Borovkov, V. V.; Sugiura, K.; Sakata, Y.; Shul'ga, A. M. *Tetrahedron Lett.* **1993**, *34*, 2153–2156.

(13) Beer, P. D.; Kurek, S. S. *J. Organomet. Chem.* **1987**, *336*, C17–C21.

(14) Dixon, D. W.; Kumar, V. *New J. Chem.* **1992**, *16*, 555–558.

(15) Gust, D.; Moore, T. A.; Moore, A. L.; Gao, F.; Luttrull, D.; DeGraziano, J. M.; Ma, X. C.; Makings, L. R.; Lee, S.-J.; Trier, T. T.; Bittersmann, E.; Seely, G. R.; Woodward, S.; Bensasson, R. V.; Rougée, M.; DeSchryver, F. C.; Van der Auweraer, M. *J. Am. Chem. Soc.* **1991**, *113*, 3638–3649.

(16) Eriksson, S.; Källebring, B.; Larsson, S.; Mårtensson, J.; Wennerström, O. *Chem. Phys.* **1990**, *146*, 165–177.

(17) Brun, A. M.; Atherton, S. J.; Harriman, A.; Heitz, V.; Sauvage, J.-P. *J. Am. Chem. Soc.* **1992**, *114*, 4632–4639. Chambron, J.-C.; Heitz, V.; Sauvage, J.-P. *J. Chem. Soc., Chem. Commun.* **1992**, 1131–1133. Brun, A. M.; Harriman, A.; Heitz, V.; Sauvage, J.-P. *J. Am. Chem. Soc.* **1991**, *113*, 8657–8663.

(18) Ashton, P. R.; Johnston, M. R.; Stoddart, J. F.; Tolley, M. S.; Wheeler, J. W. *J. Chem. Soc., Chem. Commun.* **1992**, 1128–1131.

(19) (a) Senge, M. O.; Gerzeveske, K. R.; Vincente, M. G. H.; Forsyth, T. P.; Smith, K. M. *Angew. Chem., Int. Ed. Engl.* **1993**, *32*, 750–753. Senge, M. O.; Hope, H.; Smith, K. M. *J. Chem. Soc., Perkin Trans. 2* **1993**, 11–16. Pandey, R. K.; Forsyth, T. P.; Gerzevske, K. R.; Lin, J. J.; Smith, K. M. *Tetrahedron Lett.* **1992**, *33*, 5315–5318. Pandey, R. K.; Shiau, F.-Y.; Dougherty, T. J.; Smith, K. M. *Tetrahedron* **1991**, *47*, 9571–9584. (b) Vincente, M. G. H.; Smith, K. M. *J. Org. Chem.* **1991**, *56*, 4407–4418.

0020-1669/94/1333-0972$04.50/0

dimer is highly conjugated, and it can be held planar by noncovalent interactions.

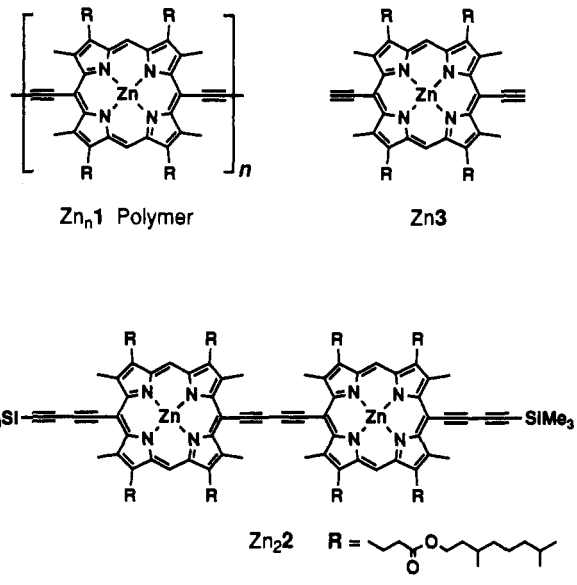

There is no steric barrier to rotation about the butadiyne links in Zn$_n$**1**, so in free solution all torsional angles should be similarly populated (Figure 1a). Formation of a double strand assembly would restrict rotation about the butadiyne links and may tend to hold the porphyrins coplanar. Two simple ways of forming a duplex can be envisaged.

(i) Two porphyrin chains may aggregate directly (Figure 1b). Porphyrins usually aggregate *via* π–π interactions.[27] Self-aggregation is strongest in porphyrins without *meso*-substituents, and in these cases the geometry is invariably parallel offset face-to-face with the center of one porphyrin lying above a pyrrole ring of the other. Linear porphyrin oligomers should aggregate in a cooperative manner, and the offset nature of the aggregation interaction should result in torsional rigidity; CPK models indicate that if the porphyrins are not coplanar they cannot aggregate.

(ii) Linear bidentate ligands may bind between pairs of metal centers to form a double strand ladder (Figure 1c). This type of binding should also be cooperative, so the ladder complex should

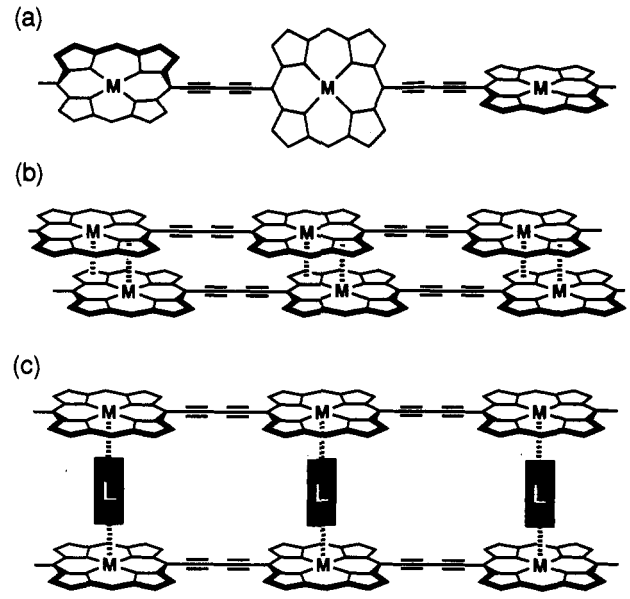

Figure 1. Torsional freedom of the Zn$_n$**1** polymer (a), which may be restricted by forming a double strand, either by aggregation (b) or by ladder complex formation (c).

self-assemble.[28] In fact any rigid ligand with *n* outwardly-pointing binding sites could undergo cooperative self-assembly with Zn$_n$**1** to form an *n*-stranded complex.

I have used NMR ring current shifts and UV exciton coupling to probe the efficiency of aggregation and ladder formation as ways of holding the model dimer, Zn$_2$**2**, coplanar. In this system aggregation strongly enforces coplanarity, whereas ladder formation allows a range of torsional angles.

The porphyrin dimer Zn$_2$**2** was investigated as a model for the synthesis, spectroscopic characteristics, and binding properties of the polymer Zn$_n$**1**. The structure of Zn$_2$**2** comprises two porphyrin units each flanked by two butadiyne units, one of which connects the two porphyrins. It represents 2.5 repeat units of Zn$_n$**1**, so it is an excellent spectroscopic model for the polymer. Zn$_2$**2** is an interesting molecule in its own right; it is a 38-Å-long rigid-rod ditopic receptor. The exciton splitting in Zn$_2$**2** is greater than that reported for any other dye in solution. It is a precursor to porphyrin polymers with alternating butadiyne and octatetrayne links.

The greatest challenge when synthesizing polymers such as Zn$_n$**1** is to make them soluble. The porphyrin dimer, Zn$_2$**2**, is a useful structure on which to test solubilizing groups. The work described in this paper used 3,7-dimethyloctyl ester sidechains. This isodecyl solubilizing group has the following advantages. (i) The alcohol is available commercially, *via* hydrogenation of terpenes. (ii) Its branched structure should destabilize packing in the solid state. (iii) It confers solubility in non-polar solvents, but not in polar ones. This facilitates crystallization. (iv) Transesterification with the racemic alcohol gives many diastereomers; for example, Zn$_2$**2** is a mixture of 55 isomers. This must improve the solubility and yet the stereocenters are so remote from the porphyrin that it does not significantly complicate the spectroscopy.

The synthesis of butadiyne-linked porphyrin polymers and oligomers such as Zn$_n$**1** and Zn$_2$**2** requires the synthesis of a porphyrin monomer, Zn**3**, with two terminal acetylene groups directly attached to opposite *meso*-positions. Porphyrins of this type have not been synthesized previously, although a porphyrin with a single ethynyl *meso*-substituent has been prepared by Arnold *et al.*[8b,29] from nickel octaethylporphyrin, *via* formylation. The obvious route to porphyrins such as Zn**3** is condensation of

(20) Collman, J. P.; Ha, Y.; Guilard, R.; Lopez, M.-A. *Inorg. Chem.* **1993**, *32*, 1788–1794. Collman, J. P.; Hutchison, J. E.; Lopez, M. A.; Tabard, A.; Guilard, R.; Seok, W. K.; Ibers, J. A.; L'Her, M. *J. Am. Chem. Soc.* **1992**, *114*, 9869–9877. Guilard, R.; Lopez, M. A.; Tabard, A.; Richard, P.; Lecomte, C.; Brandes, S.; Hutchison, J. E.; Collman, J. P. *J. Am. Chem. Soc.* **1992**, *114*, 9877–9889.

(21) Brandis, A. S.; Kozyrev, A. N.; Mironov, A. F. *Tetrahedron* **1992**, *48*, 6485–6494. Levin, E. G.; Nizhnik, A. N.; Mironov, A. F. *Mendeleev Commun.* **1992**, 95–96.

(22) Anderson, S.; Anderson, H. L.; Sanders, J. K. M. *Acc. Chem. Res.* **1993**, *26*, 469–475. Anderson, S.; Anderson, H. L.; Sanders, J. K. M. *Angew. Chem., Int. Ed. Engl.* **1992**, *31*, 907–910. Anderson, H. L.; Bonar-Law, R. P.; Mackay, L. G.; Nicholson, S.; Sanders, J. K. M. In *Supramolecular Chemistry*; Balzani, V., DeCola, L., Eds.; Kluer Academic: Dordrecht, The Netherlands, 1992; pp 359–374.

(23) (a) Kugimiya, S. *J. Chem. Soc., Chem. Commun.* **1990**, 432–434. Meier, H.; Kobuke, Y.; Kugimiya, S. *Tetrahedron Lett.* **1989**, *30*, 5301–5304. Tabushi, I.; Kugimiya, S.; Kinnaird, M. G.; Sasaki, T. *J. Am. Chem. Soc.* **1985**, *107*, 4192–4199. (b) Meier, H.; Kobuke, Y.; Kugimiya, S. *J. Chem. Soc., Chem. Commun.* **1989**, 923–924.

(24) Proniewicz, L. M.; Odo, J.; Góral, J.; Chang, C. K.; Nakamoto, K. *J. Am. Chem. Soc.* **1989**, *111*, 2105–2110. Abdalmuhdi, I.; Chang, C. K. *J. Org. Chem.* **1985**, *50*, 411–413.

(25) (a) Crossley, M. J.; Burn, P. L. *J. Chem. Soc., Chem. Commun.* **1987**, 39–40. Crossley, M. J.; Burn, P. L. *J. Chem. Soc., Chem. Commun.* **1991**, 1569–1571. (b) Kobayashi, N.; Numao, M.; Kondo, R.; Nakajima, S.; Osa, T. *Inorg. Chem.* **1991**, *30*, 2241–2244.

(26) Marcuccio, S. M.; Nevin, W. A.; Janda, P.; Kobyashi, N.; Lever, A. B. P. *J. Chem. Soc., Chem. Commun.* **1987**, 699–701. Lelièvre, D.; Bosio, L.; Simon, J.; André, J.-J.; Bensebaa, F. *J. Am. Chem. Soc.* **1992**, *114*, 4475–4479.

(27) Hunter, C. A.; Sanders, J. K. M. *J. Am. Chem. Soc.* **1990**, *112*, 5525–5534.

(28) For recent reviews on self-assembly see: Lindsey, J. S. *New J. Chem.* **1991**, *15*, 153–254. Whitesides, G. M.; Mathias, J. P.; Seto, C. T. *Science (Washington, D.C.)* **1991**, *254*, 1312–1319.

Scheme 1

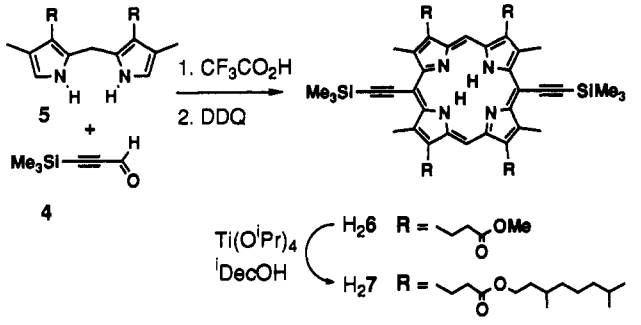

Scheme 2

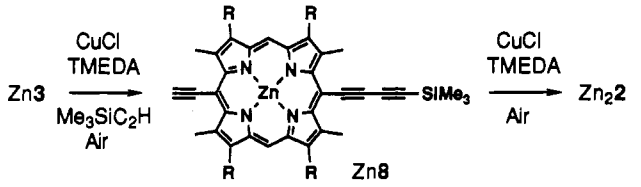

propynal with a bipyrromethane. However propynal is highly susceptible to Michael addition,[30] so I chose to use (trimethylsilyl)-propynal,[31] **4**, which behaves like a simple aldehyde.

Results and Discussion

Synthesis. (Trimethylsilyl)propynal, **4**, reacted cleanly with the bipyrromethane **5**, generated *in situ*,[32] to give a porphyrinogen which was oxidized with 2,3-dichloro-5,6-dicyano-1,4-benzoquinone to give the trimethylsilyl-protected porphyrin, H_2**6**, in 34% yield (Scheme 1).[33]

Monomeric porphyrins such as H_2**6** are very soluble in organic solvents, but the methyl ester sidechains were converted to isodecyl esters at this stage, to maintain good solubility for the dimer. Transesterification was achieved using Seebach's titanium alkoxide catalyzed conditions,[34] with isodecanol as solvent, at 100 °C/15 mmHg to strip volatile alcohols from the equilibrium. Under these conditions transesterification of all four ester groups proceeds to completion; no material with only three isodecyl sidechains was detected by FAB MS or NMR. The substituted monomer, H_2**7**, was isolated in 98% yield. Isodecyl side chains dramatically increase the porphyrin's solubility in chloroform and reduce its melting point from 288 to just 87 °C. Zinc was inserted into the porphyrin at this stage to protect it from copper metalation during Glaser–Hay coupling and the terminal acetylenes were deprotected with tetrabutylammonium fluoride to give **Zn3**.

The linear dimer Zn_2**2** was synthesized directly from **Zn3** as shown in Scheme 2. The monocapped monomer **Zn8** was isolated and characterized during preliminary studies, but not during preparative runs. **Zn3** was treated with copper(I) chloride followed by *N,N,N′,N′*-tetramethylethylenediamine (TMEDA) and excess (trimethylsilyl)acetylene,[35] to give **Zn8**. This can react further to give the biscapped compound **Zn9**, but capping of the second acetylene group occurs about 30 times more slowly than the first;[36] the electron-withdrawing effect of the first formed butadiyne substituent appears to be transmitted through the porphyrin, deactivating the second acetylene group.[37] This made it possible to stop the reaction when **Zn8** was the predominant product, remove excess (trimethylsilyl)acetylene, and reimpose Glaser coupling conditions to form the dimer Zn_2**2**, which was isolated in 28% overall yield. **Zn9** was prepared in 46% yield by coupling **Zn3** in the presence of excess trimethylsilylacetylene; it is a valuable reference compound because the porphyrin is flanked by two butadiyne groups, just as in Zn_2**2**.

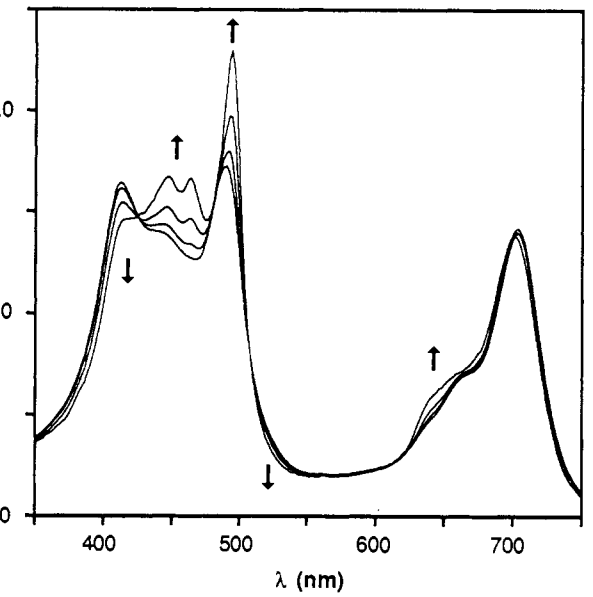

Figure 2. UV absorption spectra of Zn_2**2** in dichloromethane at 30 °C in the concentration range 10^{-5}–10^{-7} M. Arrows show change with increasing dilution.

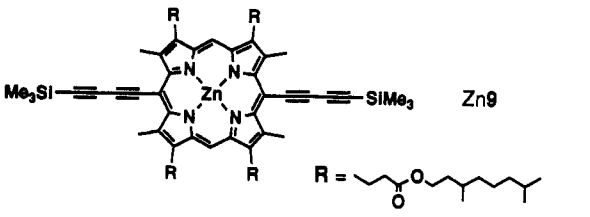

Aggregation. Equilibrium constants for the formation of bimolecular porphyrin aggregates in organic solvents are normally *ca.* 10 M^{-1} for free-base porphyrins and *ca.* 10^2 M^{-1} for their zinc complexes, so aggregation is manifest in NMR spectra (at *ca.* 10^{-3} M), but not in UV spectra (at *ca.* 10^{-6} M).[38] Linear porphyrin dimers would be expected to aggregate more strongly than monomers, so it was not surprising to find that Zn_2**2** aggregated even at the lowest concentrations accessible by UV spectroscopy. Its UV spectrum changes on dilution as shown in Figure 2, with

(29) A selenoacetal route to *meso*-tetraalkynylporphyrins has also been reported, but this has not been applied to the synthesis of porphyrins with terminal acetylene substituents: Proess, G.; Pankert, D.; Hevesi, L. *Tetrahedron Lett.* **1992**, *33*, 269–272. Palladium-catalyzed coupling of *meso*-bromoporphyrins may be an alternative route to *meso*-alkynylporphyrins: DiMagno, S. G.; Lin, V. S.-Y.; Therien, M. J. *J. Am. Chem. Soc.* **1993**, *115*, 2513–2515.

(30) Yates, P.; Douglas, S. P. *Can. J. Chem.* **1982**, *60*, 2760–2765.

(31) Komarov, N. V.; Yarosh, O. G.; Astaf'eva, L. N. *Zh. Obshch. Khim.* **1966**, *36*, 907–909. Kruithof, K. J. H.; Schmitz, R. F.; Klumpp, G. W. *Tetrahedron* **1983**, *39*, 3073–3081.

(32) Anderson, H. L.; Sanders, J. K. M. *Angew. Chem., Int. Ed. Engl.* **1990**, *29*, 1400–1403.

(33) A preliminary communication mentioning this reaction and reporting the synthesis of *meso*-tetraethynylporphyrins has been published: Anderson, H. L. *Tetrahedron Lett.* **1992**, *33*, 1101–1104.

(34) Seebach, D.; Hungerbühler, E.; Schnurrenberger, P.; Weidmann, B.; Züger, M. *Synthesis* **1982**, 138–141. Imwinkelried, R.; Schiess, M.; Seebach, D. *Org. Synth.* **1987**, *65*, 230–235.

(35) A large excess of (trimethylsilyl)acetylene was necessary because most of it couples to give bis(trimethylsilyl)butadiyne. Capping was also carried out using bromotrimethylsilylacetylene under Cadiot–Chodkiewicz conditions, but this gave less clean coupling, see: Johnson, T. R.; Walton, D. R. M. *Tetrahedron* **1972**, *28*, 5221–5236.

(36) The relative rates of formation of **Zn8** and **Zn9** were estimated from integration of signals in ^{1}H NMR spectra of crude reaction mixtures which had been quenched before coupling had gone to completion.

(37) This selectivity is surprising not just because the two acetylene groups are so far apart but also because electron-withdrawing groups normally make acetylenes more reactive to Glaser coupling; see: Klebanskii, A. L.; Grachev, I. V.; Kuznetsova, O. M. *Zh. Obshch. Khim.* **1957**, *27*, 2977–2983. Bohlmann, F.; Schönowsky, H.; Inhoffen, E.; Grau, G. *Chem. Ber.* **1964**, *97*, 794–800.

(38) White, W. I. In *The Porphyrins, Physical Chemistry, Part C*; Dolphin, D., Ed.; Academic: New York, 1978; Vol. 5, pp 303–339. Scheer, H.; Katz, J. J. In *Porphyrins and Metalloporphyrins*; Smith, K. M., Ed.; Elsevier: Amsterdam, 1975; pp 493–501.

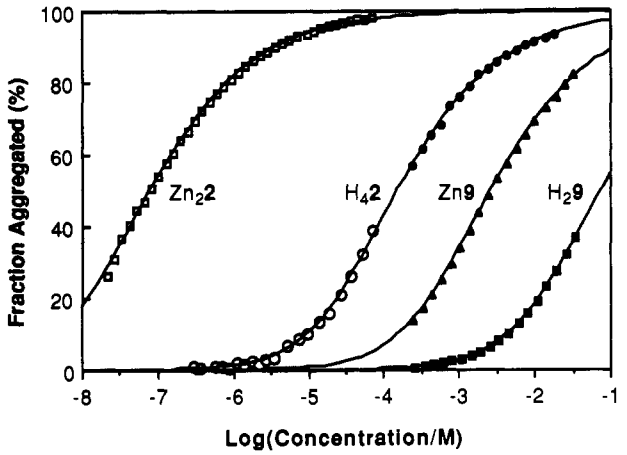

Figure 3. Aggregation curves for Zn_2**2**, H_4**2**, **Zn9**, and H_2**9** in dichloromethane at 30 °C. Data for concentrations greater than 10^{-4} M come from changes in the *meso*-proton chemical shift, whereas lower concentration data are from UV absorbance measurements. Calculated curves are for bimolecular aggregation.

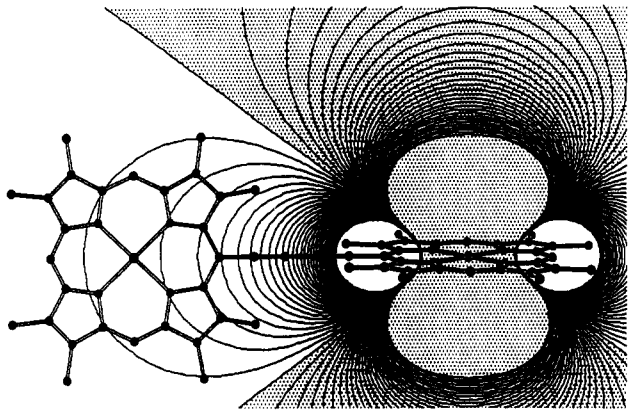

Figure 4. Contour plot showing how one porphyrin of Zn_2**2** experiences the ring current of the other porphyrin. The shaded region is shielded. Contours are at 0.1 ppm intervals in the region shifted by less than 3 ppm and were calculated using Abraham's 16 dipole model.[41] Atomic coordinates are from molecular mechanics calculations.

isosbestic points at 424, 508, 610, and 701 nm. The aggregation behavior of these compounds was thoroughly investigated using UV and ^{1}H NMR techniques.

The equilibrium constants for formation of bimolecular aggregates, K_{Agg}, for Zn_2**2**, H_4**2**, **Zn9**, and H_2**9** were found to be $1.2 \pm 0.5 \times 10^7$ M^{-1}, $7 \pm 2 \times 10^3$ M^{-1}, $3.8 \pm 0.5 \times 10^2$ M^{-1}, and 14 ± 3 M^{-1}, respectively. These binding constants were estimated by computer simulation[39] of the UV and NMR titration data; experimental and simulated curves for all four compounds are shown in Figure 3, on the same log concentration scale. The zinc dimer, Zn_2**2**, aggregates so strongly that no disaggregation can be detected by NMR; its ^{1}H NMR spectrum is concentration independent in the range 0.1–10 mM. Aggregation of the free-base dimer H_4**2** was measured using NMR and UV; both techniques gave aggregation curves consistent with a binding constant of $7 \pm 2 \times 10^3$ M^{-1}. Aggregation of the monomeric porphyrins **Zn9** and H_2**9** is much weaker and was only detected by NMR. As expected the free-base porphyrins aggregate less strongly than their zinc complexes.

The aggregation data for all four compounds fit well with the calculated curves for formation of bimolecular aggregates. The fact that Zn_2**2** shows no further aggregation in the NMR concentration range, together with the isosbesticity of the UV dilution spectra, indicate that high aggregates are less readily formed than the bimolecular aggregate. This was confirmed by vapor-phase osmometry measurements on Zn_2**2** in toluene;[40] in the concentration range 10–20 mM the apparent molecular weight was 5880 ± 900, which corresponds to a degree of oligomerization of 2.1 ± 0.3.

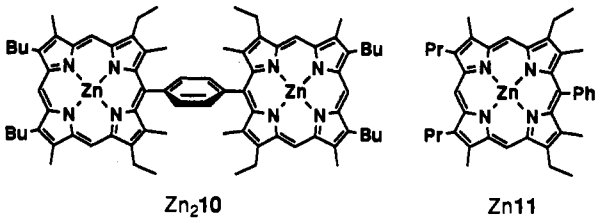

Zn_2**10** **Zn11**

Aggregation and disaggregation are fast on the NMR time scale; with Zn_2**2** only one *meso*-resonance is detected, at 9.02 ppm, even though the parallel offset $(Zn_2$**2**$)_2$ aggregate must have four distinct *meso*-environments. This dynamic behavior makes it difficult to determine the precise structure of the aggregates. However insight can be gained by comparing the chemical shifts of the dimer aggregate with those of disaggregated dimer, Zn_2**2**$(PY)_2$ (in 20% pyridine-d_5/$CDCl_3$) and by comparing the chemical shifts of dimer with those of monomer, **Zn9**. The most informative signals are those of the *meso*-proton, the ring methyls and the TMS group; these data are shown in Table 1. The chemical shifts for **Zn9**(PY) are similar to those calculated for free monomeric **Zn9** by extrapolation of dilution curves, which suggests that differences between the spectra of the pyridine complexes and the aggregates can be attributed to ring current shifts in the aggregates. Comparison of $(Zn$**9**$)_2$ with **Zn9**(PY) shows that the *meso* and ring methyl resonances are strongly shifted upfield in the aggregate, whereas the TMS resonance is shifted downfield by 0.19 ppm, showing that it lies in the deshielded region due to its greater distance from the porphyrin center. Comparison of dimer and monomer chemical shifts gives the values of $\Delta\delta$ tabulated. In all cases dimer signals are shifted downfield relative to monomer, as would be predicted from the known shape of the porphyrin ring current (Figure 4). The magnitude of the downfield shift experienced by each porphyrin in the dimer due to the porphyrin covalently attached to it depends on the relative orientation of the two porphyrin rings; the shift will be greatest when they are coplanar. The ring methyl adjacent to the central butadiyne, Me(1), is most eloquent because it experiences the greatest shift from the neighboring porphyrin.

Ring current models[41,42] can be used to predict shifts for different conformations of Zn_2**2**. For example Abraham's 16 dipole model predicts a $\Delta\delta_{Me(1)}$ of 0.3–0.4 ppm if the porphyrins are orthogonal or 0.6–0.7 ppm if they are coplanar (Figure 4). However the models are not extensively parameterized in deshielded regions of space, so it is useful to compare the ring current shifts in Zn_2**2**$(PY)_2$ and $(Zn_2$**2**$)_2$ with those of a *p*-phenylene-linked *meso*-porphyrin dimer, H_4**10**, published by Sessler et al.[6a] The porphyrins are fixed coplanar in this molecule, with a center to center distance (12.8 Å) only slightly shorter than that in Zn_2**2** (*ca.* 13.6 Å). Chemical shifts for H_4**10** and the analogous monomer, H_2**11**, are shown in Table 1.[43] $\Delta\delta_{Me(1)}$ for H_4**10** is 0.72 ppm whereas the value for Zn_2**2**$(PY)_2$ is only 0.36 ppm, indicating that, as expected, large torsional angles are well populated in the disaggregated dimer. In contrast $\Delta\delta_{Me(1)}$

(39) Saunders, M.; Hyne, J. B. *J. Chem. Phys.* **1958**, *29*, 1319–1323.

(40) A Wescor 5500 osmometer was used operating with toluene solutions at 37 °C. Zn_2**2** was compared with three reference compounds: (a) (5,15-bis(3-ethynylphenyl)-2,8,12,18-tetrakis(2-((3,7-dimethyloctanyl)-oxy)carbonyl)ethyl)-3,7,13,17-tetramethylporphinato)zinc(II), $C_{92}H_{124}N_4O_8Zn$, M_r = 1479.4; (b) methyl-7-acetoxy-12-(benzyloxy)-3-ketocholate, $C_{34}H_{48}O_6$, M_r = 552.8; (c) the cyclic trilactone of 7,-12-bis(trifluoroacetoxy)-3-hydroxycholanoic acid, $C_{84}H_{108}O_{18}F_{18}$, M_r = 1747.8. These gave effective molecular weights for Zn_2**2** of 5360 ± 600, 6440 ± 800, and 5827 ± 700, respectively. UV absorption spectra of Zn_2**2** in toluene closely resemble those in CH_2Cl_2, indicating that aggregation is similar.

(41) Abraham, R. J.; Marsden, I. *Tetrahedron* **1992**, *48*, 7489–7504. Abraham, R. J.; Bedford, G. R.; McNeillie, D.; Wright, B. *Org. Magn. Reson.* **1980**, *14*, 418–425.

(42) Cross, K. J.; Crossley, M. J. *Aust. J. Chem.* **1992**, *45*, 991–1004. Cross, K. J.; Wright, P. E. *J. Magn. Reson.* **1985**, *64*, 220–231.

Table 1. Comparison of ^{1}H NMR Chemical Shifts for Monomer and Dimer Complexes (ppm)[a]

monomer	δ_{Meso}	δ_{Me}	δ_{TMS}	dimer	δ_{Meso}	$\delta_{Me(1)}$	$\delta_{Me(2)}$	δ_{TMS}	$\Delta\delta_{Meso}$[e]	$\Delta\delta_{Me(1)}$	$\Delta\delta_{Me(2)}$	$\Delta\delta_{TMS}$
Zn**9**[b]	10.16	3.71	0.40									
Zn**9**(PY)[c]	10.10	3.69	0.38	Zn_2**2**(PY)$_2$[c]	10.13	4.05	3.72	0.39	0.03	0.36	0.03	0.01
(Zn**9**)$_2$[b]	8.77	3.37	0.57	(Zn_2**2**)$_2$	9.02	4.15	3.56	0.55	0.25	0.78	0.19	−0.02
(Zn**9**)$_2$(DABCO)[d]	9.46	3.36	0.43	(Zn_2**2**)$_2$(DABCO)$_2$	9.69	3.80	3.48	0.45	0.23	0.44	0.12	0.02
H_2**11**[f]	10.20	2.51		H_2**10**[f]	10.26	3.16			0.06	0.65		

[a] All spectra were recorded in CD_2Cl_2 unless stated otherwise. Me(1) and Me(2) are the central and end ring methyls of the dimer. [b] Calculated by extrapolation of dilution curve. [c] Measured in 20% pyridine-d_5/CD_2Cl_2. [d] Calculated by fitting titration data. [e] $\Delta\delta$ values are downfield shifts of dimers relative to monomers in analogous complexes. [f] From ref 6a (in $CDCl_3$); only signals from protons in positions analogous to those of Zn**9** and Zn_2**2** are shown.

for (Zn_2**2**)$_2$ is 0.78 ppm. Part of this large downfield shift may be due to the diagonally opposite porphyrin in the aggregate, but this contribution must be less than the 0.19 ppm shift in the TMS resonance of (Zn**9**)$_2$ relative to Zn**9**(PY) because the distance of the TMS protons to the center of Zn**9** (11–12 Å) is greater than the distance of methyl(1) to the center of the further porphyrin in Zn_2**2** (8–9 Å). Thus the shift at Me(1) of (Zn_2**2**)$_2$ due only to the covalently attached porphyrin must be 0.59–0.78 ppm, indicating that small torsional angles are preferred in the dimer aggregate. The greater value of $\Delta\delta_{Meso}$ for (Zn_2**2**)$_2$ relative to H_4**10** must be largely due to the downfield shift from the diagonally opposite porphyrin in the aggregate.

The stronger aggregation of the porphyrin dimers Zn_2**2** and H_4**2** when compared to Zn**9** and H_2**9** is clearly due to supramolecular chelation in the dimer aggregates. If, as seems likely, the microscopic aggregation properties of the porphyrin units in the dimer are the same as those in the monomer then this chelation can be quantified as an effective molarity, EM = $K_{Dimer}/(K_{Monomer})^2$. Effective molarities are useful for measuring the stabilization due to chelation in self-assembled structures and for estimating the amount of binding energy which could be used for bimolecular catalysis, if it can be directed into transition-state stabilization.[44] Zn_2**2** and H_4**2** give EM values of 80 and 40 M, respectively. These are among the highest values encountered in supramolecular complexes of this size, reflecting the tightness of these aggregates. Artificial self-replicating systems have been reported with aggregation effective molarities similar to these,[45] indicating that molecules such as Zn_2**2** and Zn_n**1** may be able to self-replicate through aggregation. It will be interesting to discover whether autocatalysis can be detected in the synthesis of Zn_2**2**.

Ladder Complex Formation. The binding of linear bidentate amine ligands to the zinc porphyrin dimer Zn_2**2** was investigated to determine whether stable ladder complexes are formed. Preliminary ^{1}H NMR titrations, in dichloromethane, with 1,4-diazabicyclo[2.2.2]octane (DABCO), 4,4′-bipiperidine (BIPIP), and 4,4′-bipyridine (BIPY) indicated that all three ligands form strong 2:2 complexes. With DABCO and BIPIP the complexes gave sharp spectra which were on slow exchange with excess porphyrin dimer, whereas with BIPY exchange was fast on the NMR time scale at 30 °C. This reflects the stronger binding of the more basic ligands.

Binding of DABCO was investigated in detail because as the shortest ligand it should give the most torsionally constrained ladder complex. Part of the ^{1}H NMR titration of Zn_2**2** with DABCO is illustrated in Figure 5. A single 2:2 complex is formed which is in slow exchange with excess Zn_2**2** but in fast exchange with excess DABCO. The simple NMR spectrum of the complex

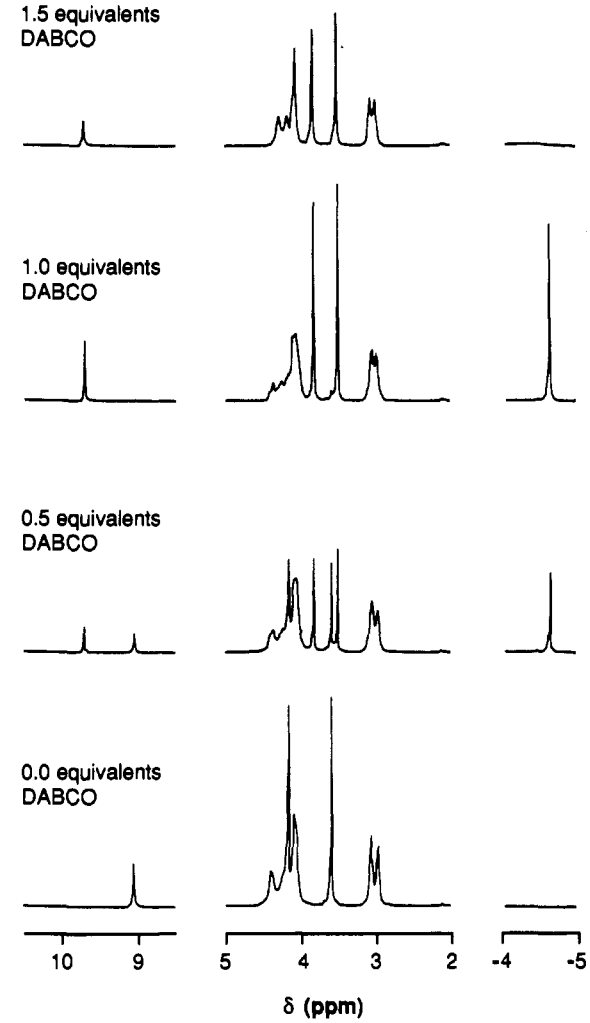

Figure 5. ^{1}H NMR spectra from a titration of Zn_2**2** (5 mM in CD_2Cl_2 at 30 °C) with DABCO.

confirms that it has a highly symmetric structure. The bound DABCO experiences a large upfield ring current shift and gives rise to a sharp singlet at −4.60 ppm. The ligand in (Zn**9**)$_2$(DABCO) resonates at −4.79 ppm; these are typical chemical shift for DABCO in this environment.[46] The sharpness of the signals due to the 2:2 complex, and the fact that they do not broaden or shift until 1 equiv of DABCO has been added proves that a discrete complex is formed. If these signals were due to a range of linear oligomeric species of the type Zn_2**2**((DABCO)-Zn_2**2**)$_n$ then a Zn_2**2**(DABCO)Zn_2**2** complex would form when $^1/_2$ equiv of DABCO had been added, and the signals would shift or broaden with the Zn_2**2**/DABCO ratio.

Comparison of the chemical shifts of (Zn_2**2**)$_2$(DABCO)$_2$ with those of (Zn**9**)$_2$(DABCO) (Table 1) show that the ring current shift at the inner ring methyl of the 2:2 complex, $\Delta\delta_{Me(1)}$, is 0.44 ppm. Up to 0.05 ppm of this shift could be due to the diagonally

(43) The chemical shifts of H_4**10** and Zn_2**2** must be influenced by many factors apart from the porphyrin ring current (such as the shielding anisotropies of the phenyl and butadiynyl groups) but these factors are the same in the monomer and in the dimer so they do not affect $\Delta\delta$. This assumes that linking the butadiyne and porphyrin units causes only a slight perturbation to their electronic structures and does not significantly affect their shielding properties.

(44) Kirby, A. J. *Adv. Phys. Org. Chem.* **1980**, *17*, 183–278. Mandolini, L. *Adv. Phys. Org. Chem.* **1986**, *22*, 1–111. Walter, C. J.; Anderson, H. L.; Sanders, J. K. M. *J. Chem. Soc., Chem. Commun.* **1993**, 458–460.

(45) Nowick, J. S.; Feng, Q.; Tivikua, T.; Ballester, P.; Rebek, J., Jr. *J. Am. Chem. Soc.* **1991**, *113*, 8831–8839.

(46) Hunter, C. A.; Meah, M. N.; Sanders, J. K. M. *J. Am. Chem. Soc.* **1990**, *112*, 5773–5780.

Scheme 3. Equilibrium for Binding DABCO to Zn_2**2**

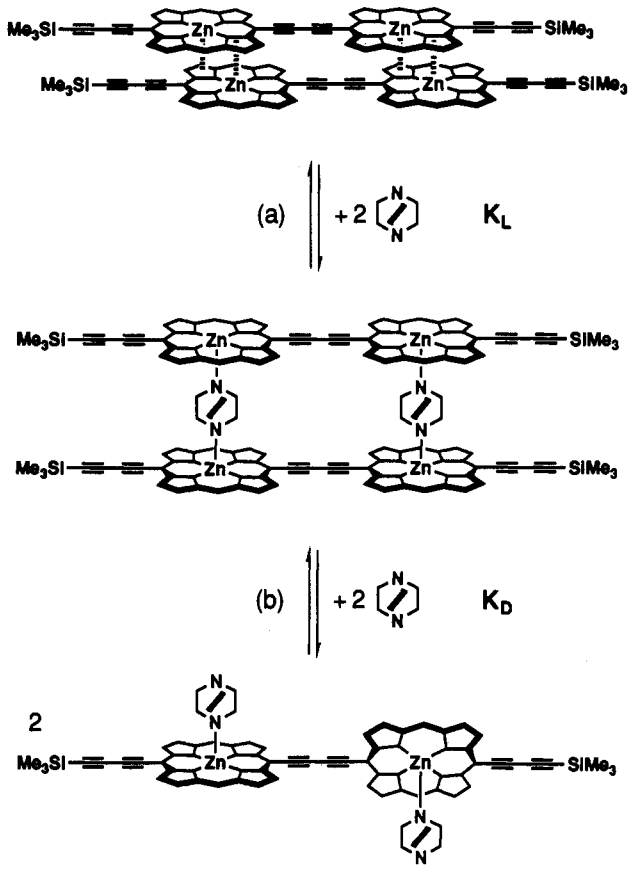

opposite porphyrin, so the shift due to the covalently attached porphyrin is 0.39–0.44 ppm. This value is only slightly greater than that in the disaggregated dimer Zn_2**2**$(PY)_2$ (0.36 ppm) which indicates that formation of the 2:2 ladder complex does not prevent the population of large torsional angles; models indicate that torsional angles as high as 45° may easily be accessible in the ladder complex because the strain can be distributed over many bonds.

The equilibrium constant for formation of the ladder complex from the aggregate, K_L (Scheme 3) is too strong to be measured at NMR concentrations. With up to 1 equiv of DABCO, the 2:2 complex was the only complex that could be detected by NMR, but as soon as more than 1 equiv of DABCO had been added, the signals due to the bound porphyrin dimer broadened and started shifting downfield. The changes in chemical shift of the *meso*-resonance as excess ligand was added gave the curve shown in Figure 6, which can be interpreted in terms of equilibrium b in Scheme 3. The system is in fast exchange, so the observed porphyrin chemical shifts are given by

$$\delta_{Mobs} = (2\delta_{M_2L_2}C_{M_2L_2} + \delta_{ML_2}C_{ML_2})/C_{Mtot} \quad (1)$$

where $\delta_{M_2L_2}$ and δ_{ML_2} are the chemical shifts of $(Zn_2\mathbf{2})_2(DABCO)_2$ and Zn_2**2**$(DABCO)_2$ respectively, and $C_{M_2L_2}$ and C_{ML_2} are the concentrations of these species, given by the cubic equation

$$4K_D{C_{M_2L_2}}^3 + 4[K_D(C_{Ltot} - 2C_{Mtot}) - 1]{C_{M_2L_2}}^2 + [K_D(C_{Ltot} - 2C_{Mtot})^2 + 4C_{Mtot}]C_{M_2L_2} - {C_{Mtot}}^2 = 0 \quad (2)$$

where C_{Mtot} is the total concentration of porphyrin dimer and C_{Ltot} is the total DABCO concentration. This equation gave a good fit to the experimental data,[47] as shown in Figure 6, for an equilibrium constant, K_D, of 60 ± 20 M^{-1}.

When DABCO binding to the reference compound **Zn9** was examined by NMR under identical conditions, the system was found to be in fast exchange on the NMR timescale at all ligand

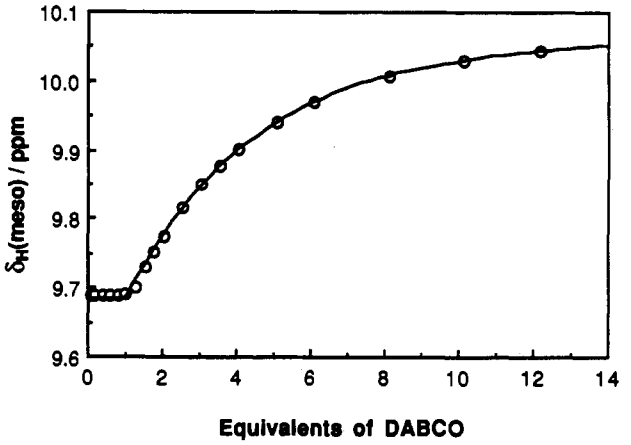

Figure 6. Change in *meso*-proton chemical shift on addition of DABCO to a 5 mM solution of Zn_2**2** in CD_2Cl_2 at 30 °C. The simulated curve is for eq 2.

Scheme 4. Equilibrium for Binding DABCO to **Zn9**

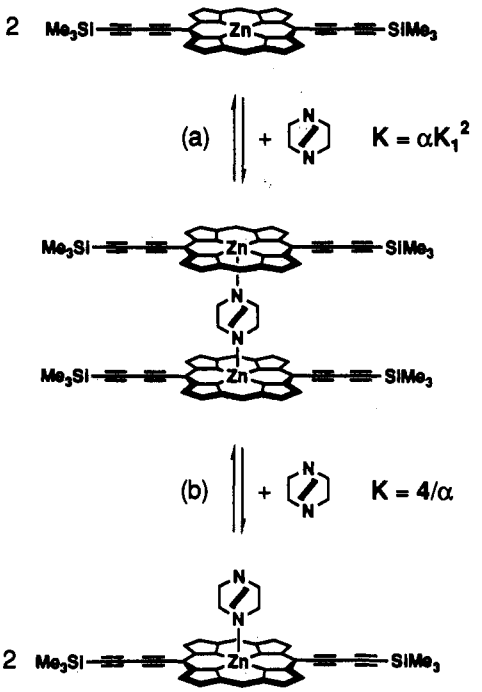

to porphyrin ratios. Until 1 equiv of DABCO had been added, it formed predominantly the sandwich complex $(Zn\mathbf{9})_2(DABCO)$, which then opened up to form the 1:1 complex with excess DABCO (Scheme 4). The initial binding constant, αK_1^2 (K_1 is the microscopic binding constant and α is the cooperativity coefficient for binding at the second end of DABCO) is too strong to measure at NMR concentrations, but the second equilibrium constant, $4/\alpha$, is weaker; simulation analysis of the binding curves[48] with excess DABCO gave a value for α of 0.9 ± 0.4, close to the statistical value.[49] This equilibrium was also studied by UV titration; under these conditions the main process is formation of

(47) The good fit obtained using this simple thermodynamic model is a consequence of the stability of the $(Zn_2\mathbf{2})_2(DABCO)_2$ complex; the curve obtained when this titration was repeated using BIPY instead of DABCO gives a much poorer fit to this equation because the $(Zn_2\mathbf{2})_2(BIPY)_2$ complex is weaker so it opens out at lower BIPY concentrations, giving rise to higher concentrations of larger complexes such as $(Zn_2\mathbf{2})_2(BIPY)_3$.

(48) The region of the binding curve after 1/2 equiv of DABCO had been added was fitted to the equation $C_{ML} = \{C_{Ltot} - [C_{Ltot}^2 + C_{Mtot}(\alpha - 1)(2C_{Ltot} - C_{Mtot})]^{1/2}\}/(1 - \alpha)$, where C_{ML} is the concentration of Zn9(DABCO), C_{Ltot} is the total DABCO concentration, and C_{Mtot} is the total concentration of Zn9. This analysis gave good fits for δ_{Meso}, δ_{Me}, δ_{TMS} and the DABCO signal, giving $\alpha = 0.9 \pm 0.4$. For a discussion of cooperativity coefficients, see: Connors, K. A.; Paulson, A.; Toledo-Velasquez, D. *J. Org. Chem.* **1988**, *53*, 2023–2026.

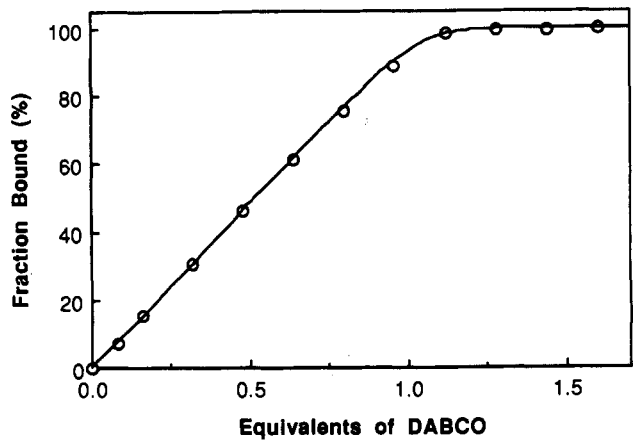

Figure 7. Binding curve for addition of DABCO to a 4 μM solution of Zn_2**2** in dichloromethane at 30 °C.

the 1:1 complex, which has a formation constant, $2K_1$, of (7.0 ± 0.7) × 10^5 M^{-1}.[50]

The UV titration binding curve for addition of DABCO to Zn_2**2** is shown in Figure 7. This titration has a clear end point at 2:2 stoichiometry. No further change is observed when a second equivalent of DABCO is added, which is consistent with the value of K_D measured by NMR; formation of the Zn_2**2**$(DABCO)_2$ complex would not be expected to become significant until 50 equiv of DABCO have been added at this concentration. This titration exhibits sharp isosbestic points at 423, 477, 483, 508, and 703 nm, which confirms that a well-defined 2:2 complex is formed, but the binding constant, K_L (Scheme 3), is too great to be measured reliably at UV concentrations (simulation analysis[51] gave a lower limit for K_L of 1.3 × 10^{14} M^{-2}). However K_L can be estimated from K_{Agg}, K_1, and K_D using the thermodynamic cycle in Scheme 5. If we assume that the microscopic binding constant of each unit in the dimer[52] is identical to that of the reference monomer, K_1, then

$$K_L = 16K_1^4/K_DK_{Agg} \quad (3)$$

which gives K_L = 3 × 10^{14} M^{-2}. Similarly K_F, the equilibrium constant for formation of $(Zn_2$**2**$)_2(DABCO)_2$ from disaggregated Zn_2**2** and DABCO, can be estimated using

$$K_F = K_LK_{Agg} = 16K_1^4/K_D \quad (4)$$

which gives K_F = 4 × 10^{21} M^{-3}. The effective molarity for

Scheme 5. Thermodynamic Cycle Used to Relate K_{Agg}, K_L, K_1, K_D, and K_F

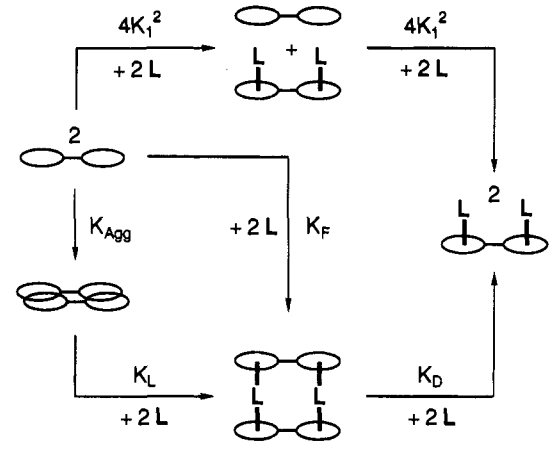

formation of the cyclic 2:2 complex can thus be calculated:

$$EM = K_{Dimer}/(K_{Monomer})^2 = K_F/(\alpha K_1^2)^2 = 16/\alpha^2K_D \quad (5)$$

This gives a value of 0.3 M, which is much lower than that of the dimer aggregate, reflecting the greater number of degrees of freedom lost on closure of the ladder complex. Nonetheless an effective molarity of 0.3 M in combination with a formation constant of 4 × 10^{21} M^{-3} means that the 2:2 complex is the dominant species present in a 1:1 mixture of Zn_2**2** and DABCO in the concentration range 0.1 μM to 100 mM; it is a remarkably stable four-component self-assembly.[53,54]

Electronic Spectra. The UV–visible–near IR absorption spectra of Zn_2**2** and H_4**2** are very different from those of the reference monomers **Zn9** and H_2**9**.[55] The magnitude of the exciton coupling is greater than can be accounted for by through-space interaction, but some qualitative features can be rationalized by the point-dipole model, using knowledge of the aggregation and binding properties. Electronic spectra of H_4**2** are slightly more complicated than those of Zn_2**2** because the NH protons reduce the symmetry, so only the zinc complexes will be discussed here.

The absorption spectra of Zn_2**2** and **Zn9** in dichloromethane at 5 × 10^{-5} M are compared in Figure 8a. Two main differences between these spectra are apparent: (i) **Zn9** gives a single sharp Soret, or B, band at 448 nm whereas Zn_2**2** gives two broad Soret peaks at 412 nm and 488 nm, and (ii) the Q band of Zn_2**2** is intensified and red-shifted by 80 nm relative to that of **Zn9**. The transition dipole moments calculated[56] from these spectra for the B and Q bands of **Zn9** are 11.9 and 5.7 D, respectively, whereas those for Zn_2**2**, per porphyrin, are 11.1 and 7.6 D. Under these conditions the dimer exists predominantly (>95%) as the aggregate, which complicates comparison of the spectra. It is not possible to record the absorption spectrum of Zn_2**2** at such low concentrations that it is predominantly disaggregated. However spectra of disaggregated Zn_2**2**$(PY)_2$ and **Zn9**(PY) can be obtained by using 1% pyridine/dichloromethane as the solvent

(49) The cooperativity for DABCO binding to rutheniumcarbonyl porphyrins, α = 0.77, is similar, see: Anderson, H. L.; Hunter, C. A.; Meah, N. M.; Sanders, J. K. M. *J. Am. Chem. Soc.* **1990**, *112*, 5780–5789.

(50) The binding constants for **Zn9** are an order of magnitude stronger than those of simple zinc porphyrins. For example pyridine and quinuclidine have binding constants of 2.2 × 10^4 M^{-1} and 7.0 × 10^5 M^{-1} respectively, in dichloromethane at 30 °C. This is presumably a result of the electron-withdrawing effect of the butadiyne groups.

(51) Consideration of equilibrium a in Scheme 3 leads to the equation $K_LC_L^3 + K_L(C_{Mtot} - C_{Ltot})C_L^2 + C_L - C_{Ltot} = 0$, where C_L is the concentration of free DABCO, C_{Ltot} is the total DABCO concentration, and C_{Mtot} is the total concentration of Zn_2**2** units. This assumes that binding is so strong that species such as Zn_2**2**(DABCO), $(Zn_2$**2**$)_2$(DABCO) and Zn_2**2**$(DABCO)_2$ are not present at significant concentrations. Simulation analysis using this equation gave the best fit for K_L = 1.3 × 10^{14} M^{-2}, but higher binding constants fit the data almost as well, so a reliable upper limit for K_L cannot be obtained from this experiment. This analysis does not directly take account of the shift in the aggregation equilibrium of Zn_2**2** during the titration. However the dimer was predominantly aggregated over the concentration range of the titration, and the wavelengths used for analysis of DABCO binding were chosen to be near the isosbestic points for the aggregation equilibrium, to minimize the effect of this complication.

(52) The binding of monodentate ligands such as pyridine and quinuclidine to Zn_2**2** is complicated; biphasic UV titration curves were obtained indicating that when a ligand binds to one end of the dimer, it causes disaggregation. It is difficult to extract reliable binding constants from these curves but they are consistent with the measured aggregation constant of 1.2 × 10^7 M^{-1} and microscopic binding constants for disaggregated dimer similar to those of **Zn9**.

(53) It is important to remember that an effective molarity of less than 1 M still corresponds to a large positive chelate effect (see ref 44).

(54) For recent examples of multicomponent self-assembly, see: Seto, C. T.; Mathias, J. P.; Whitesides, G. M. *J. Am. Chem. Soc.* **1993**, *115*, 1321–1329. Seto, C. T.; Whitesides, G. M. *J. Am. Chem. Soc.* **1993**, *115*, 1330–1340. Zimmerman, S. C.; Duerr, B. F. *J. Org. Chem.* **1992**, *57*, 2215–2217. Baxter, P.; Lehn, J.-M.; DeCian, A.; Fischer, J. *Angew. Chem., Int. Ed. Engl.* **1993**, *32*, 69–72.

(55) The butadiyne linked porphyrin dimers reported by Arnold *et al.*[8b] have UV spectra similar to that of Zn_2**2**. However these workers did not compare their porphyrin dimers with butadiyne-substituted monomers, so they did not establish which spectral characteristics are due to interactions between the porphyrin chromophores. They also did not report whether their compounds aggregate at UV concentrations.

(56) Transition dipole moments were calculated by integrating plots of extinction coefficient divided by wave number, $\epsilon(\bar{\nu})/\bar{\nu}$, versus wave number $\bar{\nu}$ and applying the equation $\mu^2 = (9.188 \times 10^{-3}/n_0)\int\{\epsilon(\bar{\nu})/\bar{\nu}\}\,d\bar{\nu}$, where n_0 is the refractive index of the solvent (1.42 for dichloromethane) and μ is the transition dipole moment in Debyes.

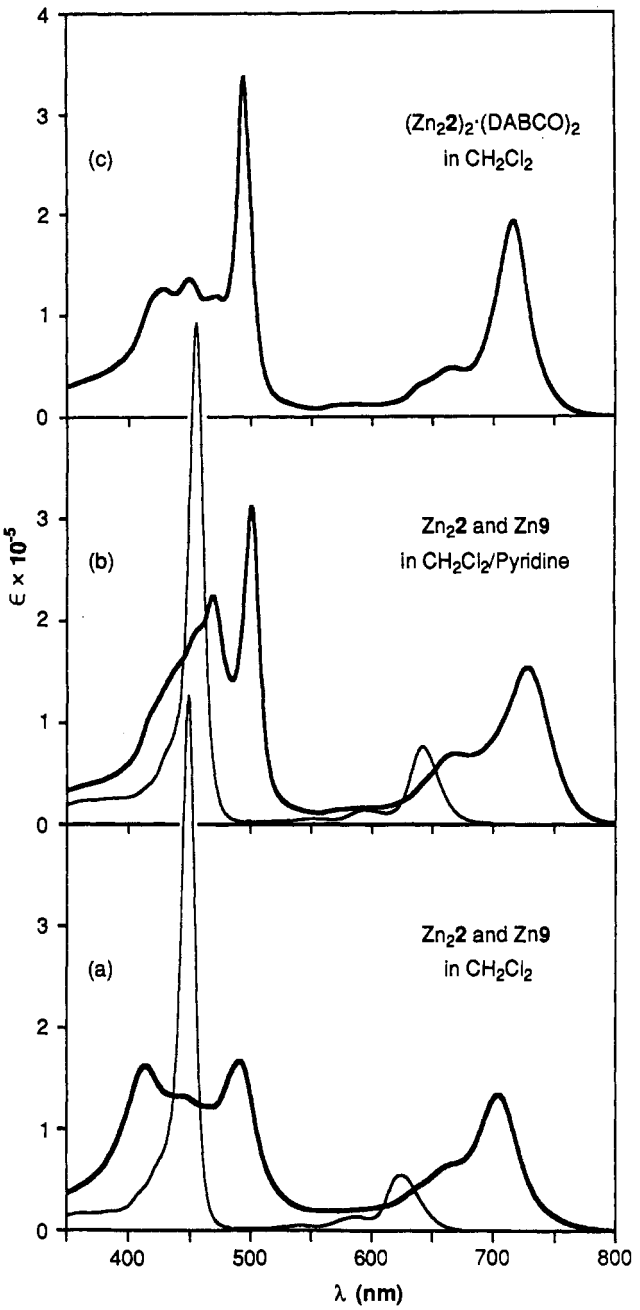

Figure 8. Electronic absorption spectra of (a) $(Zn_2\mathbf{2})_2$ (bold) and **Zn9** in dichloromethane, (b) $Zn_2\mathbf{2}(PY)_2$ (bold) and **Zn9**(PY) in 1% pyridine/dichloromethane, and (c) $(Zn_2\mathbf{2})_2(DABCO)_2$ in dichloromethane.

(Figure 8b). $Zn_2\mathbf{2}(PY)_2$ gives a dominant sharp Soret peak at 500 nm with several broader Soret peaks in the range 420–470 nm. The 2:2 ladder complex $(Zn_2\mathbf{2})_2(DABCO)_2$ gives a similar dominant red-shifted Soret at 495 nm (Figure 8c) although it also shows a significant blue-shifted component at 428 nm.

The shapes of these Soret bands can be explained by the simple point–dipole exciton coupling theory developed by Kasha.[6c,10b,11a,16,57,58] The Soret of a porphyrin has two perpendicular components B_X and B_Y. In a simple porphyrin monomer these are degenerate,[59] but in a porphyrin dimer they couple differently. For example if the porphyrins are joined along the x axis as in Figure 9, B_Y transitions are parallel and face-to-face,

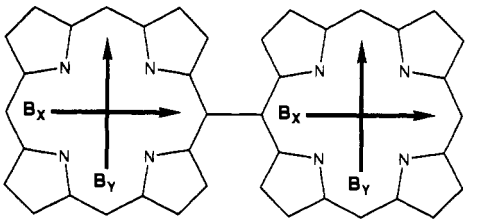

Figure 9. Soret transitions for a porphyrin dimer.

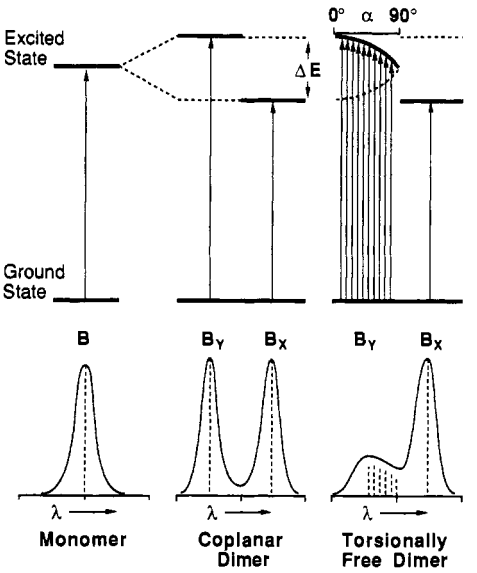

Figure 10. Kasha model for exciton coupling.

whereas B_X transitions are head-to-tail. Transition dipoles of each type couple, splitting the excited state. Transitions are only allowed to the higher energy of the two B_Y states and to the lower energy of the two B_X states. Thus the Soret band of a coplanar linear porphyrin dimer is split into a blue-shifted B_Y component and a red-shifted B_X component, Figure 10. With the point–dipole approximation, this energy splitting is given by the equation

$$\Delta E = \mu^2/2\pi\epsilon_0 R^3 \qquad (6)$$

where μ is the transition dipole moment and R is the center to center chromophore separation.[60] If the porphyrin dimer is not fixed in a coplanar conformation but can explore all possible torsional angles, α, between the two porphyrins this will broaden the blue-shifted B_Y transition because its coupling is proportional to $\mathrm{Cos}(\alpha)$ and vanishes when the two porphyrins are orthogonal.[57] However the relative orientation of the two head-to-tail B_X dipoles is unaffected by torsional angle, so B_X transitions still give rise to a sharp red-shifted Soret peak. This explains why the disaggregated dimers show a dominant sharp red-shifted Soret and a complex pattern of broader unshifted or blue-shifted Soret peaks, whereas the aggregated dimer, which is held coplanar, gives a simple split Soret. Interestingly, B_Y is slightly broader than B_X even in $Zn_2\mathbf{10}$, where the porphyrins are fixed coplanar.[6c] This is probably the result of librational broadening of the B_Y band by the effect just described.

The spectrum of the aggregate must also be influenced by intramolecular exciton coupling between face-to-face porphyrins. If the porphyrins are at van der Waals separation, 3.4 Å, this effect would result in a blue-shift of *ca* 10 nm, which explains why the red-shifted component of the aggregated dimer spectrum shifts from 488 to *ca.* 500 nm on disaggregation. The spectrum of the DABCO ladder complex resembles that of the disaggregated dimer, which implies that there is substantial torsional freedom in this complex, as indicated by NMR ring current shifts, but the

(57) Kasha, M.; Rawls, H. R.; El-Bayoumi, M. A. *Pure Appl. Chem.* **1965**, *11*, 371–392.

(58) Hunter, C. A.; Sanders, J. K. M.; Stone, A. J. *Chem. Phys.* **1989**, *133*, 395–404.

(59) The B_X and B_Y transitions cannot be exactly degenerate in **Zn9** because this monomer does not have 4-fold symmetry, but the sharpness of the Soret shows that the splitting is slight.

(60) Equation 6 can be expressed as $(\Delta\bar{\nu}/\mathrm{cm}^{-1}) = 1.0068 \times 10^4\ (\mu/\mathrm{D})^2/(R/\text{Å})^3$.

blue-shifted component is not as broad as for Zn_2**2**$(PY)_2$ which may indicate some torsional constraint.

Exciton coupling theory, which assumes no electronic overlap between chromophores, provides a qualitative explanation for some of the features of these spectra. However it does not account for the magnitude of the shifts. The center to center distance in Zn_2**2** is 13.6 Å, so eq 6 predicts that the Soret splitting should be 10 nm (490 cm^{-1}), similar to that observed in Zn_2**10** (9 nm), whereas the observed splitting is 76 nm (3.8×10^3 cm^{-1}); this is the largest exciton splitting observed for any dye in solution.[61] This splitting corresponds to an effective center to center distance of 6.9 Å and implies that the chromophores overlap on the central butadiyne.

Further evidence for electronic overlap is provided by the 80-nm shift in the Q band of Zn_2**2** relative to Zn**9**. This corresponds to a 0.2-eV reduction in the HOMO–LUMO gap. The unusually intense Q band appears to be another indication of electronic delocalization; a similar effect has been observed in edge-fused porphyrin dimers.[25b] No exciton splitting is apparent in the Q band, implying that only the red-shifted Q_X component is intensified. The possibility that this could be a charge transfer band was tested by recording the spectrum of Zn_2**2**$(PY)_2$ in solvents with different polarities. The spectrum in 1% pyridine/hexane is essentially superimposable with that in 1% pyridine/acetonitrile, proving the absence of charge transfer bands. Insight into the electronic structure of Zn_2**2** would be provided by its emission spectrum, but all attempts at detecting fluorescence from Zn_2**2** failed. Even in hexane no fluorescence could be detected over a range of concentrations, neither with nor without pyridine; the fluorescence quantum yield is less than 3×10^{-3}. This is remarkable because Zn**9** is strongly fluorescent ($\lambda_{fluor\ max}$ 640 nm, ϕ_{fluor} 0.22, in CH_2Cl_2).[62] Reduced fluorescence yields have previously been reported for short linear porphyrin dimers[21,23b,25b] and have been attributed to quenching via charge transfer states[9] and to exciton coupling.[63] It appears that in Zn_2**2** these processes are so efficient that fluorescence is undetectable.

The interaction between the porphyrin π-systems in Zn_2**2** appears to be surprisingly insensitive to torsional angle. Thus neither the magnitude of the Soret exciton coupling (as measured by the B_X red-shift), nor the shift in the Q band, nor the intensification of the Q band, nor the fluorescence quenching are any greater in coplanar $(Zn_2$**2**$)_2$ than in Zn_2**2**$(PY)_2$ or $(Zn_2$**2**$)_2$-$(DABCO)_2$. This implies that the close proximity of the two π-systems resulting from there common overlap with the central butadiyne is more important than conjugation. However if both π-systems extend over the central butadiyne then they must overlap when they are coplanar.

Summary and Conclusions

A conjugated butadiyne-linked zinc porphyrin dimer, Zn_2**2**, has been synthesized which forms a stable bimolecular aggregate and binds strongly to DABCO to give a 2:2 ladder complex. Strong evidence for the ladder complex is provided by sharp, slow-exchange NMR spectra and a cleanly isosbestic UV/visible titration. The thermodynamics of aggregation and ladder formation were explored in detail by simulation analysis of UV/visible and NMR titration curves. The NMR ring current shifts and exciton coupling interactions were elucidated by applying theoretical models (those of Abraham and Kasha respectively) and by comparison with a *p*-phenylene-linked porphyrin dimer, Zn_2**10**. Both types of interaction yielded long range information on the geometry in solution.

The properties of conjugated oligomers are strongly affected by the torsional relationship between neighboring π-systems. Can noncovalent binding be used to hold such systems coplanar? To test this idea, ring current shifts and exciton interactions were used to probe the conformations of these noncovalent assemblies. Aggregation is an excellent way of holding the porphyrins coplanar, whereas the ladder complex can twist significantly.

The electronic spectra demonstrate overlap between the porphyrin π-systems; the Soret splitting is an order of magnitude greater than predicted by point–dipole theory and the Q band is dramatically red-shifted. The synthesis of Zn_2**2** implies that the polymer, Zn_n**1**, should be accessible and soluble; it is expected to be a novel low band gap polymer. Work is underway toward the synthesis and characterization of this material.

Experimental Section

Deuterochloroform was deacidified by standing over anhydrous potassium carbonate for 24 h. Nuclear magnetic resonance spectra were recorded on a Bruker AM-400 spectrometer. UV–visible–near-IR absorption spectra were recorded in dichloromethane on a Perkin-Elmer Lambda 2 spectrometer controlled using an Amstrad PC1640. IR spectra were recorded on a Perkin-Elmer 1600 FTIR spectrometer. Fast atom bombardment (FAB) mass spectra were obtained using a *m*-nitrobenzyl alcohol matrix on a Kratos MS-50 instrument. Microanalyses were carried out by the University Chemical Laboratory Microanalysis Department in Cambridge.

All compounds were purified by flash column chromatography, using 60 mesh silica gel. Chromatographic mobility R_f values refer to chloroform elution on Merck silica gel $60F_{254}$ 0.25 mm TLC plates.

5,15-Bis(trimethylsilyl)ethynyl)-2,8,12,18-tetrakis(2-(methoxycarbonyl)ethyl)-3,7,13,17-tetramethylporphyrin ($H_2$6). Palladium on carbon (10%, 350 mg) was added to a solution of bis(5-(benzyloxycarbonyl)-3-(2-(methoxycarbonyl)ethyl)-4-methyl-2-pyrryl)methane[64] (6.14 g, 10 mmol) in THF (150 mL) containing 1% triethylamine and the mixture was stirred under hydrogen. After 1 h the catalyst was filtered off and the filtrate evaporated and redissolved in trifluoroacetic acid (TFA, 50 mL) under argon at 0 °C to generate a solution of **5**. The TFA was evaporated off over a period of 1 h, while maintaining the temperature at 0 °C. The residue was dissolved in methanol (50 mL) and treated with (trimethylsilyl)propynal, **4** (1.50 mL, 10 mmol) at −35 °C. The mixture was stirred as it warmed to −10 °C over 1 h, then oxidized with 2,3-dichloro-5,6-dicyano-1,4-benzoquinone (3.4 g, 15 mmol) at room temperature for 10 min then poured into aqueous sodium carbonate (10%, 500 mL) and extracted with chloroform. The product was purified by flash chromatography (1:1 $CHCl_3/CH_2Cl_2$) and recrystallized from dichloromethane/methanol. Yield: 34% (1.58 g). Mp: 288 °C. R_f = 0.15. FAB MS: *m/e* 902 (M^+, 1806 (M_2^+), 2710 (M_3^+). ^{1}H NMR ($CDCl_3$): δ −2.02 (s, 2H), 0.56 (s, 18H), 3.18 (t, 8H), 3.65 (s, 12H), 3.67 (s, 12H), 4.36 (t, 8H), 10.09 (s, 2H). ^{13}C NMR ($CDCl_3$): δ −0.09, 16.41, 21.74, 36.82, 51.76, 97.56, 98.09, 107.90, 110.73, 137.12, 140.10, 140.84, 147.34, 173.46; IR ($CHCl_3$): 3204 (NH), 2137 (C≡C), 1732 (CO_2R) cm^{-1}. UV, λ_{max} (log ε): 427 (5.38), 534 (4.01), 574 (4.49), 606 (3.85), 662 (4.04) nm. Anal. Calcd for $C_{50}H_{62}N_4O_8Si_2$: C, 66.49; H, 6.92; N, 6.20. Found: C, 66.27; H, 6.77; N, 6.35.

5,15-Bis((trimethylsilyl)ethynyl)-2,8,12,18-tetrakis(2-((3,7-dimethyloctanyl)oxy)carbonyl)ethyl)-3,7,13,17-tetramethylporphyrin ($H_2$7). H_2**6** (1.60 g, 1.77 mmol) was refluxed with 3,7-dimethyl-1-octanol (40 mL) and titanium(IV) isopropoxide (400 μL, 1.34 mmol) at 15 mmHg pressure/100 °C for 3 h. The excess alcohol was then distilled off under vacuum at 60 °C. Titanium alkoxides were removed from the residue by dissolving in dichloromethane (5 mL) and precipitating the porphyrin with methanol (25 mL). The product was chromatographed (CH_2Cl_2) to remove traces of low R_f material and recrystallized from dichloromethane/methanol. Yield: 98% (2.45 g). Mp: 87 °C. R_f = 0.50. FAB MS: *m/e* 1408.4 (M^+). ^{1}H NMR ($CDCl_3$): δ −1.91 (s, 2H), 0.56 (s, 18H), 0.66 (d, 12H), 0.75 (d, 24H), 0.4–1.4 (m, 40H), 3.18 (t, 8H), 3.68 (s, 12H), 4.07 (m, 8H), 4.38 (t, 8H), 10.14 (s, 2H). ^{13}C NMR ($CDCl_3$): δ −0.08, 16.47, 19.29, 21.79, 22.50, 22.59, 24.40, 27.79, 29.70, 35.38, 36.96, 37.11, 39.04, 63.24, 97.55, 98.30, 108.04, 110.57, 137.11, 140.24, 141.02, 147.41, 173.10. IR (CCl_4): 3185 (NH), 2136 (C≡C), 1734 (CO_2R) cm^{-1}. UV, λ_{max} (log ε): 428 (5.40), 534 (4.05), 575 (4.52), 606 (3.88), 663 (4.03)

(61) The largest previously reported exciton splittings, up to 70 nm (2.7×10^3 cm^{-1}), are in biscyanine dyes: Berova, N.; Gargiulo, D.; Derguini, F.; Nakanishi, K.; Harada, N. *J. Am. Chem. Soc.* **1993**, *115*, 4769–4775.

(62) Fluorescence spectra were recorded on a Shimadzu RF-5001PC spectrofluorophotometer. Fluorescence quantum yields were calibrated with tetraphenylporphyrin in benzene (ϕ_{fluor} 0.11): Seybold, P. G.; Gouterman, M. *J. Mol. Spectry.* **1969**, *31*, 1–13.

(63) Tran-Thi, T. H.; Lipkier, J. F.; Maillard, P.; Momenteau, M.; Lopez-Castillo, J. M.; Jay-Gerin, J.-P. *J. Phys. Chem.* **1992**, *96*, 1073–1082.

(64) Clezy, P. S.; Liepa, A. J. *Aust. J. Chem.* **1970**, *23*, 2443–2459.

nm. Anal. Calcd for $C_{86}H_{134}N_4O_8Si_2$: C, 73.35; H, 9.59; N, 3.98. Found: C, 73.16; H, 9.69; N, 3.82.

[5,15-Bis((trimethylsilyl)ethynyl)-2,8,12,18-tetrakis(2-((3,7-dimethyloctanyl)oxy)carbonyl)ethyl)-3,7,13,17-tetramethylporphinato]zinc-(II) (Zn7). A solution of H_27 (2.00 g, 1.42 mmol) in THF (40 mL) was refluxed with zinc acetate dihydrate (640 mg, 2.92 mmol) under argon for 2 h. The solvent was then evaporated and the product recrystallized from methanol at −20 °C. Yield: 99% (2.06 g). Mp: 80–81 °C. R_f = 0.21. FAB MS: m/e 1472 (M^+), 2941 (M_2^+). ^{1}H NMR ($CDCl_3$): δ 0.57 (s, 18H), 0.67 (d, 12H), 0.74 (d, 24H), 0.7–1.5 (m, 40H), 3.13 (t, 8H), 3.70 (s, 12H), 4.08 (m, 8H), 4.32 (t, 8H), 9.93 (s, 2H). ^{13}C NMR ($CDCl_3$): δ 0.14, 17.59, 19.30, 21.62, 22.47, 22.56, 24.37, 27.77, 29.70, 35.37, 36.89, 36.94, 39.01, 63.07, 97.59, 109.45, 110.79, 137.80, 140.48, 143.55, 148.97, 173.03. IR (CCl_4): 2137 (C≡C), 1735 (CO_2R) cm^{-1}. UV, λ_{max} (log ε): 434 (5.71), 572 (4.20), 607 (4.36) nm. Anal. Calcd for $C_{86}H_{132}N_4O_8Si_2Zn$: C, 70.19; H, 9.04; N, 3.81. Found: C, 70.12; H, 9.09; N, 3.66.

[5,15-Bis(ethynyl)-2,8,12,18-tetrakis(2-((3,7-dimethyloctanyl)oxy)carbonyl)ethyl)-3,7,13,17-tetramethylporphinato]zinc(II) (Zn3). Tetrabutylammonium fluoride (1 M in THF, 2.72 mL, 2.72 mmol) was stirred with a solution of Zn7 (2.00 g, 1.36 mmol) in dichloromethane (50 mL) for 15 min then the product was neutralized with acetic acid (160 μL, 2.80 mmol), chromatographed to remove traces of low R_f byproduct, and recrystallized once from methanol and then again from hexane. Yield: 89% (1.60 g). Mp: >300 °C dec. R_f = 0.16. FAB MS: m/e 1327.4 (M^+). ^{1}H NMR ($CDCl_3$): δ 0.64 (d, 12H), 0.73 (d, 24H), 0.5–1.4 (m, 40H), 2.99 (t, 8H), 3.59 (s, 12H), 4.03 (m, 8H), 4.22 (t, 8H), 4.56 (s, 2H), 9.52 (s, 2H). ^{13}C NMR ($CDCl_3$): δ 17.28, 19.30, 21.58, 22.49, 22.58, 24.40, 27.79, 29.72, 35.39, 36.88, 36.97, 39.03, 63.10, 87.40, 93.72, 96.34, 97.64, 137.85, 140.60, 143.84, 149.09, 173.10. IR (CCl_4): 3308 (C≡C–H), 2092 (C≡C), 1734 (CO_2R) cm^{-1}. UV, λ_{max} (log ε): 428 (5.58), 568 (4.13), 611 (4.24). Anal. Calcd for $C_{80}H_{116}N_4O_8Zn$: C, 72.40; H, 8.81; N, 4.22. Found: C, 72.38; H, 8.95; N, 4.13.

1,4-Bis[(15-((trimethylsilyl)butadiynyl)-2,8,12,18-tetrakis(2-((3,7-dimethyloctanyl)oxy)carbonyl)ethyl)-3,7,13,17-tetramethylporphyrin-5-yl)butadiynato]dizinc(II) (Zn_22). TMEDA (5.48 mL, 36.3 mmol) was added to a mixture of Zn3 (100 mg, 75 μmol), trimethylsilylacetylene (520 μL, 3.69 mmol) and copper(I) chloride (4.00 g, 40.4 mmol) in dichloromethane (1.20 L). The mixture was stirred vigorously under dry air for 20 min and then quenched with water (1 L). The organic layer was washed with water until all the copper had been removed, evaporated, and chromatographed (7% $CHCl_3/CH_2Cl_2$). The crude monocapped intermediate (Zn8) was then dissolved in dichloromethane (150 mL), stirred with copper(I) chloride (500 mg, 5.05 mmol) and TMEDA (685 μL, 4.54 mmol) for 25 min, and then washed as previously, chromatographed (25% $CHCl_3/CH_2Cl_2$), and recrystallized from dichloromethane/methanol. Yield: 28% (30 mg). Mp: >300 °C. R_f = 0.13. FAB MS: m/e 2844 (M^+), 1423 (M^{2+}). ^{1}H NMR ($CDCl_3$): δ 0.53 (s, 18H), 0.6–1.5 (m, 152H), 2.92 (t, 8H), 3.00 (t, 8H), 3.54 (s, 12H), 4.02 (m, 16H), 4.09 (s, 12H), 4.17 (m, 8H), 4.37 (m, 8H), 9.00 (s, 4H). ^{13}C NMR ($CDCl_3$): δ 0.25, 16.88, 17.93, 19.20, 19.28, 21.60, 21.70, 22.41, 22.49, 22.50, 22.58, 24.30, 24.37, 27.69, 27.77, 29.64, 29.70, 35.32, 35.38, 36.64, 36.88, 36.96, 38.94, 39.04, 63.09, 81.01, 89.91, 91.21, 91.63, 91.88, 95.56, 95.72, 98.19, 98.27, 137.62, 137.88, 140.28, 140.41, 143.09, 143.28, 149.06, 149.80, 173.05, 173.12. IR (CCl_4): 2182 (C≡C), 2127 (C≡C), 2092 (C≡C), 1734 (CO_2R) cm^{-1}. UV, λ_{max} (log ε): 413 (5.21), 491 (5.22), 703 (5.15) nm. Anal. Calcd for $C_{170}H_{246}N_8O_{16}Si_2Zn_2$: C, 71.78; H, 8.72; N, 3.92. Found: C, 71.98; H, 8.86; N, 3.84.

1,4-Bis(15-((trimethylsilyl)butadiynyl)-2,8,12,18-tetrakis(2-((3,7-dimethyloctanyl)oxy)carbonyl)ethyl)-3,7,13,17-tetramethylporphyrin-5-yl)-butadiyne (H_42). A solution of Zn_22 (70 mg, 0.025 mmol) in chloroform (10 mL) was stirred with TFA (200 μL) for 2 min and then washed with water (2 × 200 mL), evaporated, chromatographed (25% $CHCl_3/CH_2Cl_2$), and recrystallized from dichloromethane/methanol. Yield: 94% (63 mg). Mp: >300 °C dec. R_f = 0.18. FAB MS: m/e 2717 (M^+). ^{1}H NMR ($CDCl_3$): δ −4.09 (s, 4H), 0.54 (s, 18H), 0.6–1.5 (m, 152H), 2.99 (t, 8H), 3.05 (t, 8H), 3.51 (s, 12H), 3.86 (s, 12H), 4.07 (m, 24H), 4.18 (m, 8H), 9.12 (s, 4H). ^{13}C NMR (CD_2Cl_2): δ 0.15, 15.90, 16.56, 19.32, 19.38, 21.57, 21.71, 22.52, 22.60, 22.68, 24.69, 24.73, 28.08, 28.14, 30.07, 35.77, 36.91, 37.03, 37.29, 37.31, 39.34, 39.39, 63.37, 63.41, 80.34, 89.60, 89.68, 90.86, 90.93, 94.68, 95.69, 96.61, 98.17, 136.06, 136.20, 139.01, 139.19, 140.67, 140.87, 146.85, 147.53, 173.09, 173.13. IR (CCl_4): 3190 (NH), 2184 (C≡C), 2128 (C≡C), 2091 (C≡C), 1733 (CO_2R) cm^{-1}. UV, λ_{max} (log ε): 4.18 (5.27), 454 (5.35), 484 (5.38), 644 (4.95), 724 (5.23) nm. Anal. Calcd for $C_{170}H_{250}N_8O_{16}Si_2$: C, 75.12; H, 9.27; N, 4.12. Found: C, 75.38; H, 9.38; N, 4.06.

[5,15-Bis((trimethylsilyl)butadiynyl)-2,8,12,18-tetrakis(2-((3,7-dimethyloctanyl)oxy)carbonyl)ethyl)-3,7,13,17-tetramethylporphinato]zinc-(II) (Zn9). TMEDA (5.48 mL, 36.3 mmol) was added to a mixture of Zn3 (100 mg, 75 μmol), (trimethylsilyl)acetylene (320 μL, 2.27 mmol) and copper(I) chloride (4.00 g, 40.4 mmol) in dichloromethane (1.20 L). The mixture was stirred vigorously under dry air for 1 h, with addition of (trimethylsilyl)acetylene (80 μL, 0.57 mmol each 2.5 min) during the first 30 min. The mixture was then quenched with water (1 L) and washed until all the copper had been removed, evaporated, chromatographed (5% $CHCl_3/CH_2Cl_2$), and recrystallized from dichloromethane/methanol. Yield: 46% (52 mg). Mp: 122 °C to a mesophase[65] clearing at 199 °C. R_f = 0.23. FAB MS: m/e 1519 (M^+), 3037 (M_2^+). ^{1}H NMR ($CDCl_3$): δ 0.43 (s, 18H), 0.62 (d, 12H), 0.72 (d, 24H), 0.7–1.4 (m, 40H), 3.04 (t, 8H), 3.58 (s, 12H), 4.03 (m, 8H), 4.20 (t, 8H), 9.62 (s, 2H). ^{13}C NMR ($CDCl_3$): δ 0.09, 16.67, 19.25, 21.43, 22.46, 22.55, 24.35, 27.76, 29.67, 35.35, 36.75, 36.93, 39.00, 63.07, 80.78, 89.50, 90.75, 95.43, 95.81, 98.57, 137.97, 140.80, 144.07, 150.07, 172.95. IR (CCl_4): 2183 (C≡C), 2090 (C≡C), 1734 (CO_2R) cm^{-1}. UV, λ_{max} (log ε) 448 (5.66), 588 (4.08), 623 (4.67) nm. Anal. Calcd for $C_{90}H_{132}N_4O_8Si_2Zn$: C, 71.14; H, 8.76; N, 3.69. Found: C, 71.13; H, 8.90; N, 3.64.

5,15-Bis((trimethylsilyl)butadiynyl)-2,8,12,18-tetrakis(2-((3,7-dimethyloctanyl)oxy)carbonyl)ethyl)-3,7,13,17-tetramethylporphyrin (H_29). A solution of Zn9 (50 mg, 0.033 mmol) in chloroform (10 mL) was stirred with TFA (500 μL) for 5 min and then washed with water (2 × 200 mL), evaporated, chromatographed (CH_2Cl_2), and recrystallized from dichloromethane/methanol. Yield: 96% (46 mg). Mp: 176–177 °C. R_f = 0.58; FAB MS: m/e 1455 (M^+). ^{1}H NMR (CD_2Cl_2): δ −3.03 (s, 2H), 0.48 (s, 18H), 0.63 (d, 12H), 0.76 (d, 24H), 0.5–1.4 (m, 40H), 3.06 (t, 8H), 3.51 (s, 12H), 4.06 (m, 8H), 4.16 (t, 8H), 9.61 (s, 2H). ^{13}C NMR (CD_2Cl_2): δ −0.08, 15.82, 19.29, 21.72, 22.53, 22.61, 24.64, 28.08, 29.94, 35.64, 37.03, 37.19, 39.30, 63.33, 79.92, 89.12, 89.12, 89.92, 95.40, 95.84, 99.03, 136.60, 140.30, 141.44, 148.08, 173.06. IR (CCl_4): 3198 (NH), 2185 (C≡C), 2092 (C≡C), 1734 (CO_2R) cm^{-1}. UV, λ_{max} (log ε): 440 (5.53), 557 (4.06), 596 (4.83), 6.78 (4.42) nm. Anal. Calcd for $C_{90}H_{134}N_4O_8Si_2$: C, 74.23; H, 9.28; N, 3.85. Found: C, 74.27; H, 9.39; N, 3.80.

Binding constants were determined in CD_2Cl_2 (dried and deacidified over anhydrous $CaCl_2/K_2CO_3$) or CH_2Cl_2 (distilled off CaH_2) at 30 ± 0.5 °C, by means of ^{1}H NMR or UV titration, using microliter syringes. Binding curves were analyzed using a Simplex nonlinear curve-fitting program, with a combination of bisection and the Newton–Raphson method for iteratively solving polynomial equilibrium expressions.[66] Stock solutions of DABCO were made up with freshly sublimed material and used within 3 h of preparation; this is important because nucleophilic attack of the solvent becomes significant after this time.

Acknowledgment. I am grateful to Magdalene College, Cambridge, U.K., for funding and to Jeremy Sanders for generous provision of facilities. I also thank Sally Anderson, Richard Bonar-Law, Arno Kraft, and Christopher Hunter for stimulating discussion, and the SERC mass spectrometry service (Swansea, U.K.) for FAB mass spectra.

(65) Zn9 forms two discotic mesophases which have been characterized by X-ray diffraction: Anderson, H. L.; Hanna, S. Submitted for publication.

(66) Press, W. H.; Flannerly, B. P.; Teukolsky, S. A.; Vetterling, W. T. *Numerical Recipes in Pascal*; Cambridge University: Cambridge, U.K., 1989.